Bangladesh J. Bot. **55**(2): 387-394, 2026 (June) DOI: .....

ASSOCIATION OF *FUSARIUM CHLAMYDOSPORUM* FRONT WITH WILT DISEASE OF BLACK CUMIN AND ITS MANAGEMENT

SUMITRA DEY, FARHANA RAHMAN*, MD MANIRUZZAMAN SIKDER, MD SABBIR AHMED AND NUHU ALAM

Laboratory of Mycology and Plant Pathology, Department of Botany, Jahangirnagar University, Savar, Dhaka-1342, Bangladesh

Keywords: Nigella sativa, Fusarium chlamydosporum, Antagonistic fungi, *In silico*

Abstract

The present study identified the pathogenic fungus causing wilt disease in black cumin through morphological, molecular, and pathogenicity analyses, and evaluated *in vitro* and *in silico* disease management strategies. The isolated fungus produced white to pink colonies with septate, branched, woolly mycelia; obovoid, aseptate microconidia; and slightly curved macroconidia with 3-4 septa. Molecular identification based on the ITS region (507bp) confirmed the pathogen as *Fusarium chlamydosporum* (GenBank Accession No. PP002077.1), supported by phylogenetic analysis using the neighbor-joining method. Rovral TS 26WP and Tilt 250EC completely inhibited fungal growth, while *Trichoderma harzianum* and *T. erinaceum* showed strong antagonistic activity. Molecular docking identified the phytocompound epoxy azadiradione with the highest binding affinity, a stability further validated by 100 ns Molecular Dynamics simulations. These results suggest that epoxy azadiradione may serve as a promising lead compound for future antifungal development and need further validation through experiments. This is the first report of *F. chlamydosporum* causing wilt on black cumin in Bangladesh, and it introduces a pioneering combined *in vitro* and *in silico* framework for managing this emerging fungal disease.

Introduction

Black cumin (*Nigella sativa* L.) a member of the Ranunculaceae family is a medicinally significant aromatic plant. It is also known as black seed, black sesame, kaljeera, fennel flower, and nutmeg flower (Datta *et al*. 2012). The Bangladesh Agricultural Research Institute has produced a new high yielding variety of black cumin as- BARI Kalozira-1 that can be grown throughout Bangladesh during the Rabi season (Roy *et al*. 2023). Bangladesh produces 1005 million tons of black cumin from 862 hectre land of Sariatpur, Pabna, Bogra, Faridpur, Sirajganj, Madaripur, Rangpur, Jessore, Natore and Kustia districts. The utilization of black cumin has been prevalent in traditional medicinal practices and considered as a remedy for every illness (Yimer *et al*. 2019).

The yield of black cumin is impacted by several fungal diseases such as wilt, damping off, foot and root rot. Several *Fusarium* species have been linked to black cumin, and they include *F. oxysporum, F. solani*, *F. camptoceras, F. lateritium*, and *F. moniliforme* (Khaledi and Hassani 2021). Now a days phytopathogenic fungus causing wilt diseases are a serious threat for crop production all over the world (Rahman *et al*. 2024).

Various biocontrol approaches and techniques are becoming more popular for controlling fungal plant disease (Sultana *et al*. 2020). Natural phyto-compounds have been shown to be successful in controlling plant diseases, and they may be a safe substitute for chemical fungicides. Various formulations based on phytocompounds have been developed and are now available for commercial use (Elgharbawy *et al*. 2020).

Mitogen-activated protein kinases (MAPKs) are essential elements of signal transduction process in plants and fungi (Jiang *et al.* 2018). In phytopathogenic fungi, MAPK signaling

*Author for correspondence: <farhana@juniv.edu>.

pathways regulate infection-related development, virulence, and adaptation to environmental stress, making them attractive targets for antifungal discovery. Fungal MAPKs facilitate the mechanical or enzymatic penetration into the host plants during interactions between plants and phytopathogenic fungi, whereas plant MAPKs play an important role in the activation of plant immunity (Hamel *et al*. 2012). To date, no published reports have documented *Fusarium chlamydosporum* as the causal agent of wilt disease of black cumin in Bangladesh. Therefore, the objectives of this study were to investigate the causal pathogen through morphological and molecular approaches, control it *in vitro*, and explore potential antifungal phytocompounds through molecular docking and molecular dynamics simulation targeting fungal MAPK.

Materials and Methods

Infected plants showing typical wilt symptoms were collected from commercial black cumin fields in Manikganj, Dhaka, Bangladesh. Surface-sterilized stem tissues (0.2 × 0.2 cm) were cultured on PDA at 28 ± 2°C for fungal isolation. Colony morphology and mycelial structures were examined for preliminary identification (Barnett and Hunter 2000). For molecular identification, genomic DNA was extracted from 10-day-old cultures using the Promega Wizard DNA extraction kit. PCR amplification was performed using universal ITS primers ITS1F and ITS4R, and the purified products were sequenced (First BASE Laboratories, Malaysia). The obtained sequence was submitted to NCBI for accession and analyzed using BLASTn, while phylogenetic relationships were inferred using the neighbor-joining method (Tamura *et al*. 2013). Pathogenicity was confirmed via Koch's postulates under *in vivo* conditions (Ahmmed *et al*. 2022).

Three commercial fungicides-Amistar Top 325SC (Azoxystrobin + Difenoconazole), Rovral TS 26WP (Iprodione + Carbendazim 52.5%), and Tilt 250EC (Propiconazole) - were evaluated at different concentrations against the radial growth of the fungus. Dual culture technique was employed to assess the antagonistic efficacy of *Trichoderma harzianum* and *T. erinaceum* against the fungi. Radial growth inhibition (%) was calculated following the method described by Rahman *et al.* (2025).

The targeted protein MAPK sequence, as an amino acid length is retrieved in FASTA format along with the GenBank accession number from Uniprot and was used to create the 3D structure of the selected protein. The Galaxy WEB server was employed to generate the 3D structure of the specified protein, which employs an optimization-driven refinement approach alongside multiple templates to rectify inaccuracies in termini or loops. Subsequently, the initial protein model underwent refinement through the Galaxy Refine server. Based on RMSD, GDT-HA, MolProbity score, weak rotamers, clash score, and Rama preference, the best refined model was selected.

The proteins and phytocompounds three-dimensional structures underwent standard optimization within UCSF Chimera software, ensuring their integrity in the widely recognized PDB format. The CASTp server predicted the active site of the target protein. Docking computes, the binding free energy between the ligand and receptor and determines the configurations espoused around the binding sites of macromolecular targets (Ferreira *et al*. 2015). The grid centers for docking were set at coordinates X= 36.088, Y= 103.946 and Z= 11.577 for the targeted protein while the grid box dimensions were X= 50, Y= 40, Z= 40, with a spacing of 0.375 Å between each grid point. The molecular docking analysis of the targeted protein with the most promising natural phytocompounds was conducted using Autodock Vina.

To prioritize phytocompounds with potential effectiveness against the targeted protein for biogenic fungicide development, their fungicide likeness parameters based on SWISS ADME were assessed (Daina *et al*. 2017). Lipinski's rule of 5 specifies that for a compound to be considered favorable for fungicide likeness, it should fall within certain thresholds: MW ≤500

Dalton, logP ≤5, HBA ≤10, and HBD ≤5 (Peng *et al.* 2014). To examine structural rigidity and validate the docking scenarios of the best ligand-protein complexes, alongside the reference compound, molecular dynamics simulations were conducted for 100 ns. In the Linux operating system, Desmond was employed to identify the two protein-ligand complexes exhibiting the highest binding energy, alongside a control complex. To assess the stability of the complexes, the RMSD and RMSF values were analyzed. The stability of the ligand-protein complex was assessed by analyzing the RMSD value. Likewise, notable fluctuations in RMSD were observed throughout the simulation period for the protein-ligand complex in comparison to the protein-control complex.

Standard statistical analysis tools, including MS Excel, SPSS 20, MEGA 11.0, and the BLAST tool, were employed to evaluate the data generated throughout the research. The data were examined using one-way ANOVA accompanied by Duncan's post-hoc test within SPSS-20.

Results and Discussion

The oldest leaves wilted first, followed by the younger ones that develop symptoms in a systematic way. Plants wither and perish when they reach a height of 2.5-5.0 cm. Leaves' color changes from green to yellow (Fig. 1A). During the advanced phases, the plant's tips and leaves droop, ultimately resulting in the complete death of the plants. Depending on the culture medium, the fungal colony was white and circular, and it started to turn pink in color with aging (Fig. 1B). Mycelium was branched, septate, with a smooth margin and woolly in appearance. Microconidia were single, obovoid in shape, with no septation, and they were produced from elaborate polyphialides that result in branching conidiophores with a tree-like appearance, while macroconidia were slightly curved with 3-4 septation (Fig. 1C). A chlamydospore was observed during the microscopic examination (Fig. 1D). The above morphological features suggested that the isolated fungus could be *F. chlamydosporum*. This species is known to produce a lot of white, fluffy mycelium, especially when it is cultivated on nutrient-rich media like PDA.

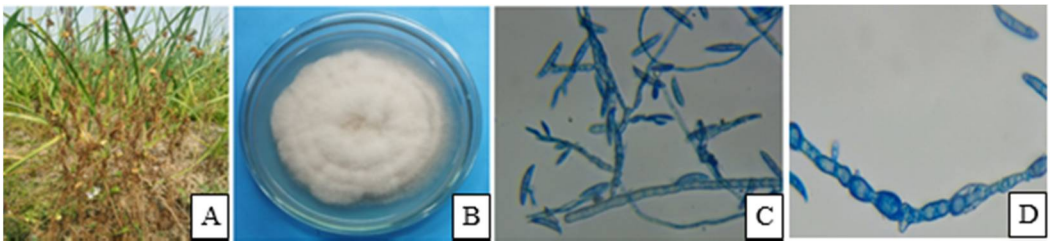

Fig. 1. A: Infected black cumin plants, B: Colony of *Fusarium chlamydosporum*, C: Mycelium with conidiophore and conidia, and D: Chlamydospore.

The PCR product amplicon size was about 507bp. The resulting sequence data were then submitted to the National Centre for Biotechnology Information (NCBI) to obtain an accession number. The NCBI processed the ITS sequencing data for *F. chlamydosporum* and assigned it the accession number PP002077.1 (JUF00074). The isolated fungus was identified as *F. chlamydosporum* through a BLASTn search analysis. The nucleotide sequence of the ITS region was utilized to construct a phylogenetic tree that encompasses 26 representative species of *Fusarium*, including *F. chlamydosporum* and an outgroup, *Claviceps purpurea* (FM952769.1). In this phylogenetic representation, the taxa are organized into five major clades (Fig. 2).

The sequence alignment led to the construction of a phylogenetic tree, which confirmed the identity of the fungus as *F. chlamydosporum* that clustered with other taxa of *F. chlamydosporum*

and belongs to the family Nectriaceae. This significant resemblance supports previous morphological identification and validates the pathogen's species-level identity (Alam and Rahman 2020). These findings are consistent with earlier research in which *F. chlamydosporum* was consistently identified from a variety of hosts, including orchids, using ITS sequencing (Siddiquee *et al.* 2010).

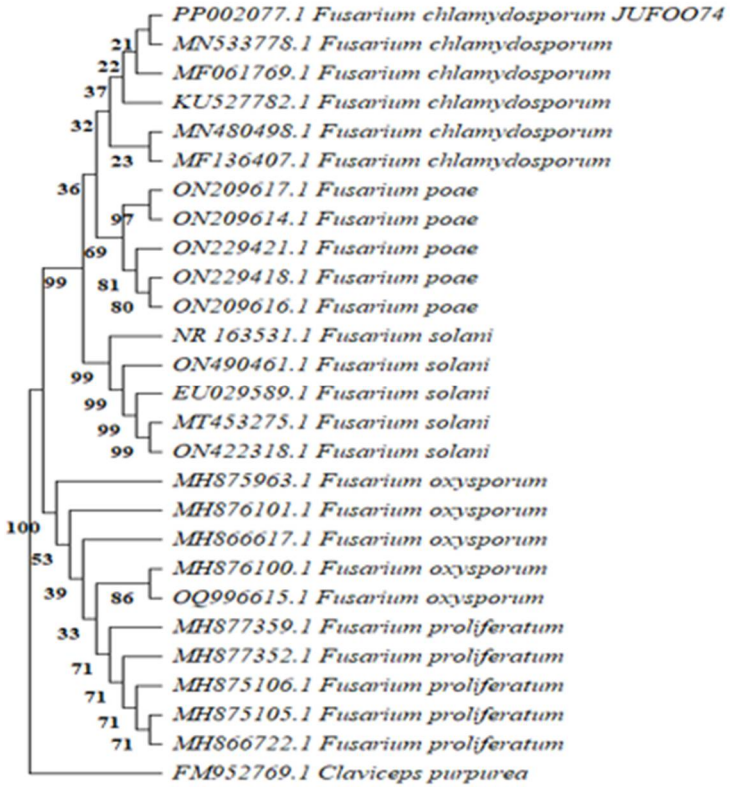

Fig. 2. Phylogenetic tree of the fungi obtained through neighbor-joining method with 1000 bootstrapping.

Trichoderma species are found as an effective biocontrol agent against *F. chlamydosporum* that causes wilt disease. *Trichoderma harzianum* and *T. erinaceum* showed 67 and 63% growth inhibition of *F. chlamydosporum,* respectively, in the current study. Rovral TS and Tilt showed the complete growth inhibition in all the tested concentrations. Besides, Amistar Top 750 and 500 ppm showed 85% and 80% growth inhibition, respectively (Fig. 3).

Yassin *et al*. (2021) studied the antagonistic effect of *T. viride* and *T. harzianum* against *F. chlamydosporum* which caused disease in *Sorghum biocolor*. *Trichoderma harzianum* has significantly higher inhibitory activity against *F. chlamydosporum*. Another investigation of fungicide effectiveness on *F. chlamydosporum* was done by Buttar *et al*. (2023).

In the current study for *in silico* experiment Mitogen activated protein kinase (Uniprot accession number M9UVX2) was selected as the targeted protein from the *F. chlamydosporum*. Ten phytocompounds were selected from several medicinal plants based on their antifungal activity. Among them three compounds - azadiradione (-7.5), baicalein (-7.2), gedunin (-7.2) showed a higher binding affinity than the control (difenoconazole) (-7.1) and epoxy azadiradione

(-7.5) containing the highest result. It also contains fungicide likeness properties. Several other factors such as hydrogen bond with the targeted protein and further analysis through MD simulation was carried out to check the stability of the selected compound with the targeted protein. The RMSD and RMSF values of epoxy azadiradione- MAP kinase complex showed a strong correlation with high stability over MAP kinase-control complex. This phytocompound from *Azadirachta indica* may represent a promising lead candidate for antifungal development against *F. chlamydosporum.* However, its efficacy should be validated through *in vitro* antifungal assays, greenhouse trials, and field evaluations before any conclusions regarding practical disease management can be drawn. Although MAPK pathways are evolutionarily conserved among eukaryotes, fungal MAPKs play critical roles in virulence, host invasion, and stress adaptation. The present docking analysis identifies epoxy azadiradione as a potential inhibitor of fungal MAPK; however, additional comparative docking, selectivity analyses, and experimental validation are required to determine its specificity toward fungal MAPKs relative to homologous proteins in plants and animals.

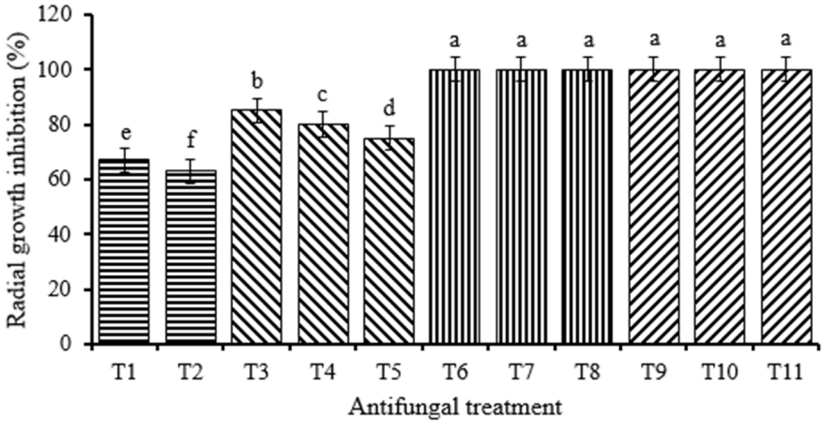

Fig. 3. Effects of different antifungal agents on *Fusarium chlamydosporum*. T1: *Trichoderma harzianum*, T2: *T. erinaceum*, T3: Amistar top 750 ppm, T4: Amistar top 500 ppm, T5: Amistar top 250 ppm, T6: Rovral 1000 ppm, T7: Rovral 750 ppm, T8: Rovral 500 ppm, T9: Tilt 300 ppm, T10: Tilt 200 ppm, T11: Tilt 100 ppm. The bars in the Fig. indicate means ± the standard errors (n = 3). Different letters in each treatment indicate significant differences at $p < 0.05$.

Five refined models were obtained from the GalaxyWEB server for the targeted protein of the fungus. From these five refined models, model 5 was selected for subsequent experiments. Model 5 showed 100% Ramachandran favor, 0.9801 GDT-HA value, 0.302 RMSD value, MolProbity 1.583, Clash score 11.7, and Poor Rotamers value 0.7. The Ramachandran plot from the SAVES server validates the protein structure, which revealed 95.5% favored zone of the residues (Fig. 4A). Several active sites were found in the targeted protein where ligands were preferred to dock were marked as red colored pocket (Figs 4B, C). In order to predict their binding interaction, selected compounds were docked with the targeted protein through Autodock Vina.

The stabilization of phytocompounds binding affinity with the protein binding site is known to relay on the presence of H-bonds and other bonded interactions in the molecular docked complexes. In this study, Epoxy azadiradione showed the highest binding score with the targeted protein. It produced two H-bonds with the target protein's amino acids in positions 119 and 146 (Fig. 4D). On the other hand, control produced one H bond with 144 amino acids of the protein (Fig. 4E).

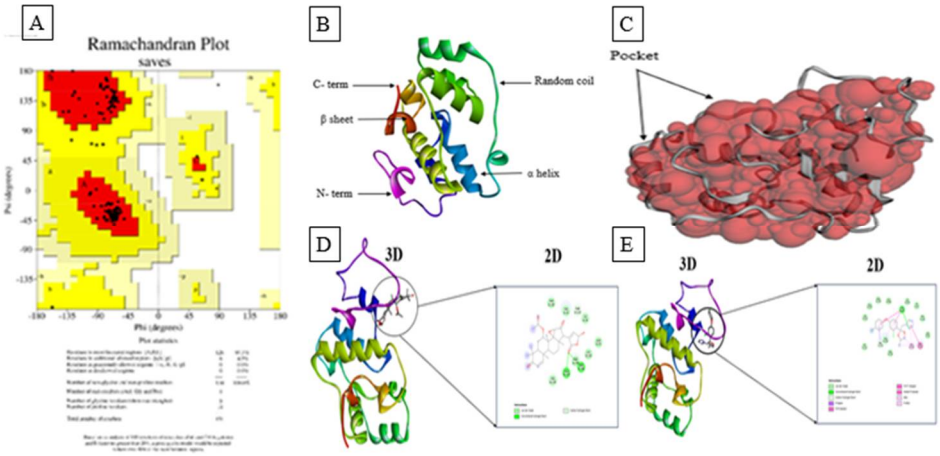

Fig. 4. PROCHECK analysis of RAMACHANDRAN plot showing 95.5% favored areas (A), Visualization of the 3D structure of the target protein **(**B**),** and binding sites of the target protein (C), 3D and 2D diagram of interaction of the best docked complex. Docking results show the interactions of Epoxy-azadiradione (D), and Difenoconazole (E) with the active side of the target protein, MAPkinase.

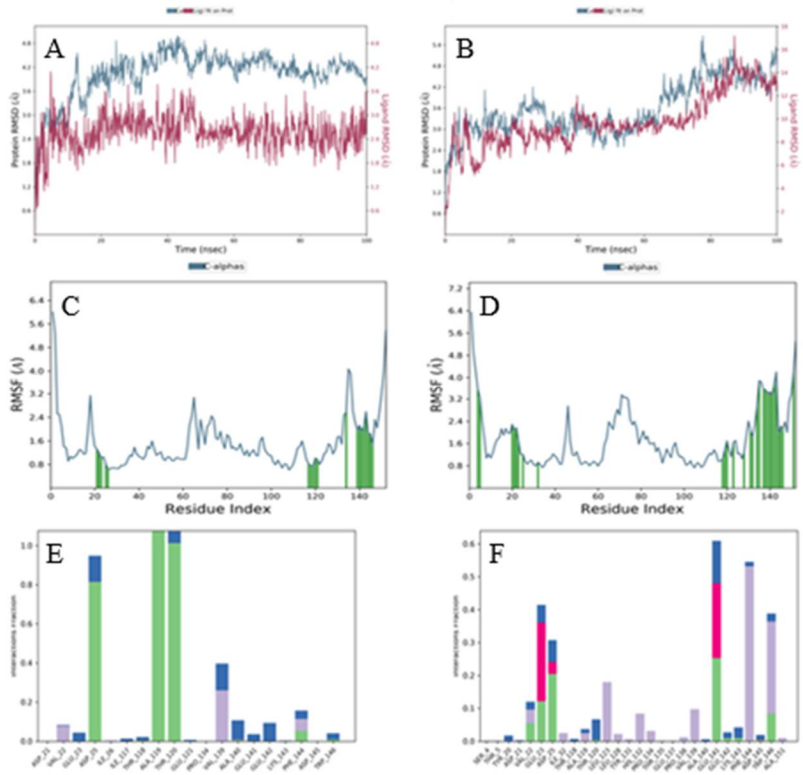

Fig. 5. Simulation graph of RMSD and RMSF values of the protein-ligand complexes. A: Picture shows the RMSD value of the protein (MAPk)-ligand (Epoxy azadiradione) complex. B: Picture shows the RMSD of the protein (MAPk)-control (difenoconazole) complex. C: RMSF value for the protein (MAPk)-ligand (Epoxy azadiradione) complex. D: RMSF value for the protein (Epoxy azadiradione)-control (difenoconazole) complex. E and F: Histogram of protein-ligand complexes.

To confirm the stability of the ligands in the protein's active site, a 100-ns dynamic simulation was carried out on the targeted protein with the best-performing ligand, epoxy azadiradione, and reference compound, difenoconazole. Several hydrogen bonds, RMSD, and RMSF value were also evaluated to confirm the consistency. In the mitogen-activated protein kinase- epoxy azadiradione complex, the RMSD average value for the protein stabilized around 3.5-4.1 Å after ~20 ns (Fig. 5A). It indicates that the protein reached a relatively stable conformation during the simulation. For Ligand RMSD**,** it fluctuated between 0.6 and 2.0 Å, remaining relatively stable and low (Fig. 5A). It suggested strong binding stability of the ligand within the protein's active site. In the mitogen-activated protein kinase-control (difenoconazole) complex, Protein RMSD started lower (~2.5 Å) but increased and fluctuated significantly after 60 ns, reaching up to 5.5 Å, suggesting less structural stability or possible conformational changes over time. For ligand RMSD, it increased steadily throughout the simulation, rising to ~16 Å and implying ligand displacement or unbinding from the protein binding site (Fig. 5B).

The RMSF values of the mitogen-activated protein kinase-epoxy azadiradione complex show a slight structural fluctuation with high stability compared to the mitogen-activated protein kinase-difenoconazole complex (control) in MD simulation (Figs 5C, D). Good RMSD and RMSF values were found in the mitogen-activated protein kinase–epoxy azadiradione complex than in the mitogen-activated protein kinase–difenoconazole complex. The ligand interacted with ALA119 and TRP146 amino acid positions of the protein, whereas the control interacted with PHE144 amino acid (Figs 5E, F).

Joshi *et al.* (2021) conducted an *in silico* study in which phytochemicals from *Melia azedarach* were screened through molecular docking against the target protein isocitrate lyase (ICL) of *Fusarium graminearum*, a key enzyme for fungal survival. Fourteen phytocompounds showed strong binding affinity with the bacterial peptide deformylase (PDF) protein, among which bisdemethoxycurcumin exhibited the highest binding energy. Additionally, nimbinene, melianoninol, fraxinellone, and vilasinin demonstrated satisfactory binding activity. Similarly, cucurbitacin 1 and curcumerin A showed strong docking scores against the QNE4 protein of *Pseudoperonospora cubensis*, the causal agent of cucumber downy mildew (Jhansirani *et al.* 2023). In this context, *in silico* methods may serve as an effective strategy for developing environmentally friendly fungicides derived from phytocompounds.

References

Ahmmed MS, Nisha FA and Alam N 2022. First report on rhizome rot disease of *Curcuma longa* caused by *Fusarium solani* in Bangladesh. American J. Plant Sci. **13**(4): 506-516.

Alam N and Rahman F 2020. Vegetative growth and genetic diversity in different strains of *Pleurotus salmoneastramineus* based on PCR polymorphism. Bangladesh J. Bot. **49**(1): 125-134.

Barnett HL and Hunter BB 2000. Illustrated Genera of Imperfect Fungi. 4th edn. Burgess Pub. Co., Minneapolis. pp. 218.

Buttar HS, Singh A, Sirari A, Kaur K, Kumar A, Lal MK, Tiwari RK and Kumar R 2023. Investigating the impact of fungicides and mungbean genotypes on the management of pod rot disease caused by *Fusarium equiseti* and *Fusarium chlamydosporum*. Front. Plant Sci. **14**: 1164245.

Daina A, Michielin O and Zoete V 2017. Swiss ADME: a free web tool to evaluate pharmacokinetics, drug-likeness and medicinal chemistry friendliness of small molecules. Sci. Rep. **7**(3): 42717.

Datta AK, Saha A, Bhattacharya A, Mandal A, Paul R and Sengupta S 2012. Black cumin (*Nigella sativa* L.)-a review. J. Plant Dev. Sci. **4**(1): 1-43.

Elgharbawy A, Samsudin N, Zuhanis Y, Hashim Y, Salleh H, Santhanam J and Ben Belgacem F 2020. Phytochemicals with antifungal properties: Cure from nature. Malays. J. Microbiol. **16**(4): 10.21161/mjm.

Ferreira LG, Dos Santos RN, Oliva G and Andricopulo AD 2015. Molecular docking and structure-based drug design strategies. Molecules **20**(7): 13384-13421.

Hamel LP, Nicole MC, Duplessis S and Ellis BE 2012. Mitogen-activated protein kinase signaling in plant-interacting fungi: distinct messages from conserved messengers. Plant Cell. **24**(4):1327-1351.

Jhansirani N, Devappa V, Sangeetha CG, Sridhara S, Shankarappa KS and Mohanraj M 2023. Identification of potential phytochemical/antimicrobial agents against *Pseudoperonospora cubensis* causing downy mildew in cucumber through *in-silico* docking. Plants **12**(11): 1-26.

Jiang C, Zhang X, Liu H and Xu JR 2018. Mitogen-activated protein kinase signaling in plant pathogenic fungi. PLoS Pathog. **14**(3):e1006875.

Joshi T, Joshi T, Sharma P, Pundir H and Chandra S 2021. *In silico* identification of natural fungicide from *Melia azedarach* against isocitrate lyase of *Fusarium graminearum*. J. Biomol. Struct. Dyn. **39**(13): 4816-4834.

Khaledi N and Hassani F 2021. Effect of seed-borne *Fusarium* species on constituents of essential oils from seeds of black cumin populations. J. Plant Protect. Res. **61**(3): 229-242.

Peng QX, Guan XH, Yi ZG and Su YP 2015. *In silico* approaches in anesthetic drug development: computer-aided drug designing. Drug Res. **65**(11): 587-591.

Rahman F, Dey S, Alam NB, Bhowmik DD, Alam N and Alam N 2025. Mycelial growth and molecular identification of pathogenic fungi isolated from basal rot disease of onion. Plant Tiss. Cult. Biotech. **35**(1): 93-104.

Rahman F, Sumitra D and Alam N 2024. Pathogenic fungi associated with coriander wilt disease: cultural condition, molecular identification and biological control. Plant Tiss. Cult. Biotech. **34**(2): 193-204.

Roy S, Islam MA, Rahman MM and Sarkar MN 2023. Effect of different fertilizer levels on yield performance of black cumin in Brahmaputra and Jamuna floodplain soil of Bangladesh. J. Biosci. Agric. Res. **31**(1): 2589-2597.

Siddiquee S, Yusuf UK and Zainudin NAIM 2010. Morphological and molecular detection of *Fusarium chlamydosporum* from root endophytes of *Dendrobium crumenatu.* African J. Biotechnol. **9**(26): 4081-4090.

Sultana S, Sikder MM, Ahmmed MS, Sultana A and Alam N 2020. Mycelial growth and biological control measures of *Botrytis cinerea* isolated from strawberry fruit rot disease in Bangladesh. Univ. J. Microbiol. Res. **8**(2): 13-18.

Tamura K, Stecher G, Peterson D, Filipski A and Kumar S 2013. MEGA6: molecular evolutionary genetics analysis version 6.0. Mol. Biol. Evol. **30**(12): 2725-2729.

Yassin MT, Mostafa AAF and Al-Askar AA 2021. *In vitro* antagonistic activity of *Trichoderma harzianum* and *T. viride* strains compared to carbendazim fungicide against the fungal phytopathogens of *Sorghum bicolor* (L.) Moench. Egypt. J. Biol. Pest Con. **31**(1): 1-9.

Yimer EM, Tuem KB, Karim A, Ur-Rehman N and Anwar F 2019. *Nigella sativa* L. (Black cumin): a promising natural remedy for wide range of illnesses. Evid. Based Complement. Altern. Med. **6**: 1-16.

(Manuscript received on 20 November, 2025; revised on 02 June, 2026)